Available online at www.sciencedirect.com
SCIENCE DIRECT®
Journal of Geochemical Exploration 77 (2003) 25–43
JOURNAL OF GEOCHEMICAL EXPLORATION
www.elsevier.com/locate/jgeoexp

Dahab stream sediments, southeastern Sinai, Egypt: a potential source of gold, magnetite and zircon

A.A. Surour*, A.A. El-Kammar, E.H. Arafa, H.M. Korany

Department of Geology, Faculty of Science, Cairo University, Giza, Egypt

Received 30 September 2002

Abstract

The stream sediments of Dahab area, southeastern Sinai, Egypt, were studied for their content of economic minerals. These sediments are immature as indicated by poor sorting and other mechanical parameters. They are derived from Precambrian basement rocks, which are mostly represented by granitic rocks in addition to lesser amounts of volcanics and gabbros. The mineralogical investigation revealed that these sediments contain considerable amounts of placer gold, Fe–Ti oxides and zircon.

The concentrated Fe–Ti oxides comprise homogeneous magnetite and ilmenite in addition to ilmeno-magnetite, hemo-ilmenite and rutile–hematite intergrowths. Isodynamic separation of some raw samples of size = 1 mm revealed that up to 15.12% magnetic minerals can be recovered. Zircon shows remarkable variations in morphology, colour, chemistry and provenance. U-poor and U-rich varieties of zircon were discriminated containing UO_2 in the ranges of 0.04–1.19 and 3.05–3.68 wt.%, respectively. REE-bearing minerals comprise monazite, allanite and La-cerianite.

On mineralogical basis, the present work suggests that Dahab stream sediments represent a promising target for further geochemical exploration for precious metals, especially gold. Fire assay data indicate that placer gold in the studied sediments sometimes reaches 15.34 g/t. Narrow gullies and valleys cutting the basement manifest the development and preservation of gold in this arid environment. Background concentration of gold and variation in lithology suggest multiple source of the metal in the investigated sediments.

Keywords: Placer gold; Zircon; Stream; Dahab; Egypt

1. Introduction

The Precambrian rocks of Sinai are highly dissected by dry valleys that are filled by a wide variety of stream sediments. The Arabic term ‘‘wadi’’ is always dedicated to dry streams and hence the expression ‘‘wadi deposits’’ is sometimes used instead of ‘‘stream sediments’’.

In this paper, the mechanism of gold dispersion in arid environments is studied in order to characterize their placer gold and associated heavy minerals. Regardless the type of environment, the mechanism of gold dispersion is controlled by environmental and paleoenvironmental factors in addition to nature of the source rocks from which gold is derived. Very little information on placer gold of arid environment is known, but some useful contributions were made by Bogoch et al. (1993) and Herail et al. (1999) who studied the effect of geomorphological factors on the

* Corresponding author.
E-mail address: aasurour63@hotmail.com (A.A. Surour).

0375-6742/02/$ - see front matter © 2002 Elsevier Science B.V. All rights reserved.
doi:10.1016/S0375-6742(02)00268-6

concentration of gold in the placers of southern Israel and the Atacama Desert in Chile, respectively. The present paper sheds more light on the effect of source rocks on the dispersion of gold in the arid environments in terms of grain size, background values and source multiplication. Understanding of the behaviour of gold dispersion in arid regions has its emphasis on the style of geochemical exploration because such regions are characterized by low-geochemical activity and dominancy of mechanical weathering. Also, the paper investigates and evaluates the potentiality of Dahab stream sediments, southeastern Sinai (Fig. 1), in terms of by-product materials such as rare-earth elements and radioactive minerals. One of the main aims of the article is the correlation between composition of the stream sediments and their Precambrian source rocks in the hinterland.

Careful survey of relevant literature indicates that nothing has been published on the economics of stream deposits in Sinai except for white glass sands (Khalid and Oweiss, 1995a). Exploration programs of the Geological Survey of Egypt revealed that gold in Sinai is confined to quartz veins and carbonated ultramafics that were considered as "*listwanite*" (Khalid and Oweiss, 1995b). On the other hand, gold in quartz veins and placers has been known in the Eastern Desert of Egypt since time of the Pharaohs.

2. Geological set up: Precambrian rocks and stratigraphy

Geomorphologically, the area to the west and south of Dahab town is characterized by its rugged topography that has been formed due to continuous erosion and development of the drainage pattern. A composite aerial photograph of Dahab, which is located on the Gulf of Aqaba (Fig. 1), is given in order to show the vast aerial distribution of the Precambrian rocks in comparison with the costal alluvial fans of probable Neogene age. The Precambrian rocks of Dahab are traversed by numerous wadis that have been surveyed for their stream sediments (Fig. 2a). Generally, the Precambrian rocks of Dahab area are mostly represented by felsic and mafic plutonites (El-Metwally et al., 1999). Beyth et al.

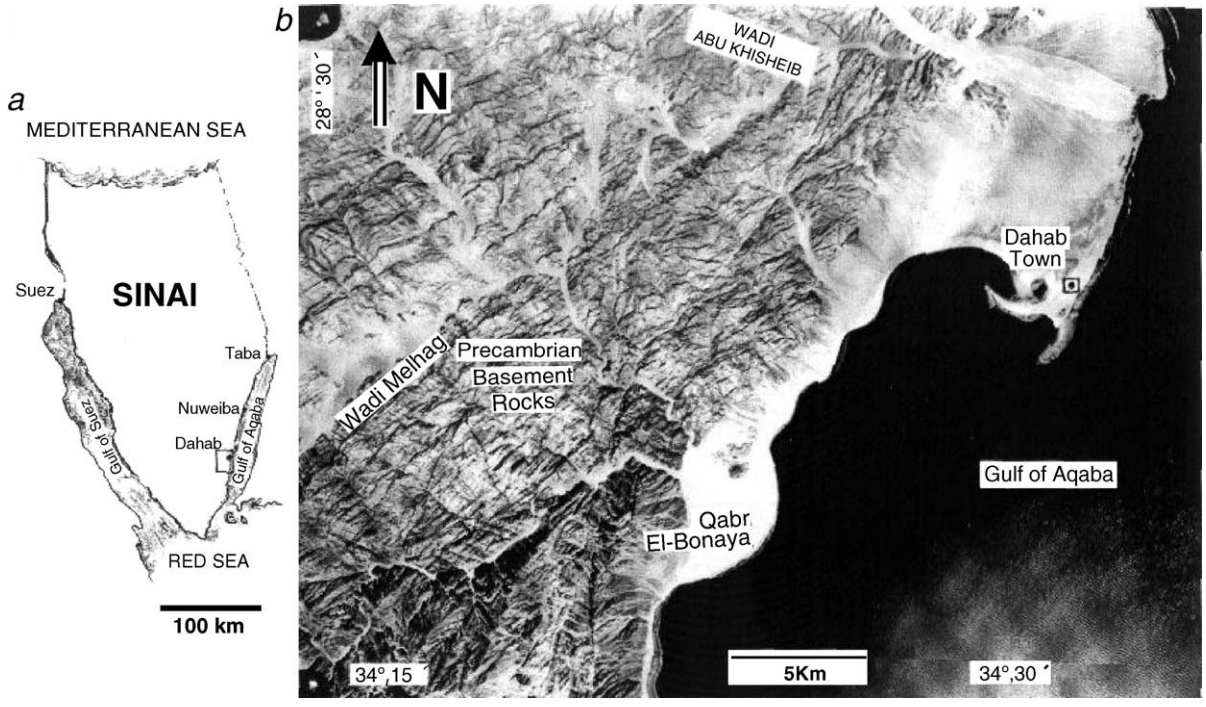

Fig. 1. (a) Location map of Dahab area. (b) Aerial photograph showing the Precambrian rocks, main streams and alluvial fans of Dahab area.

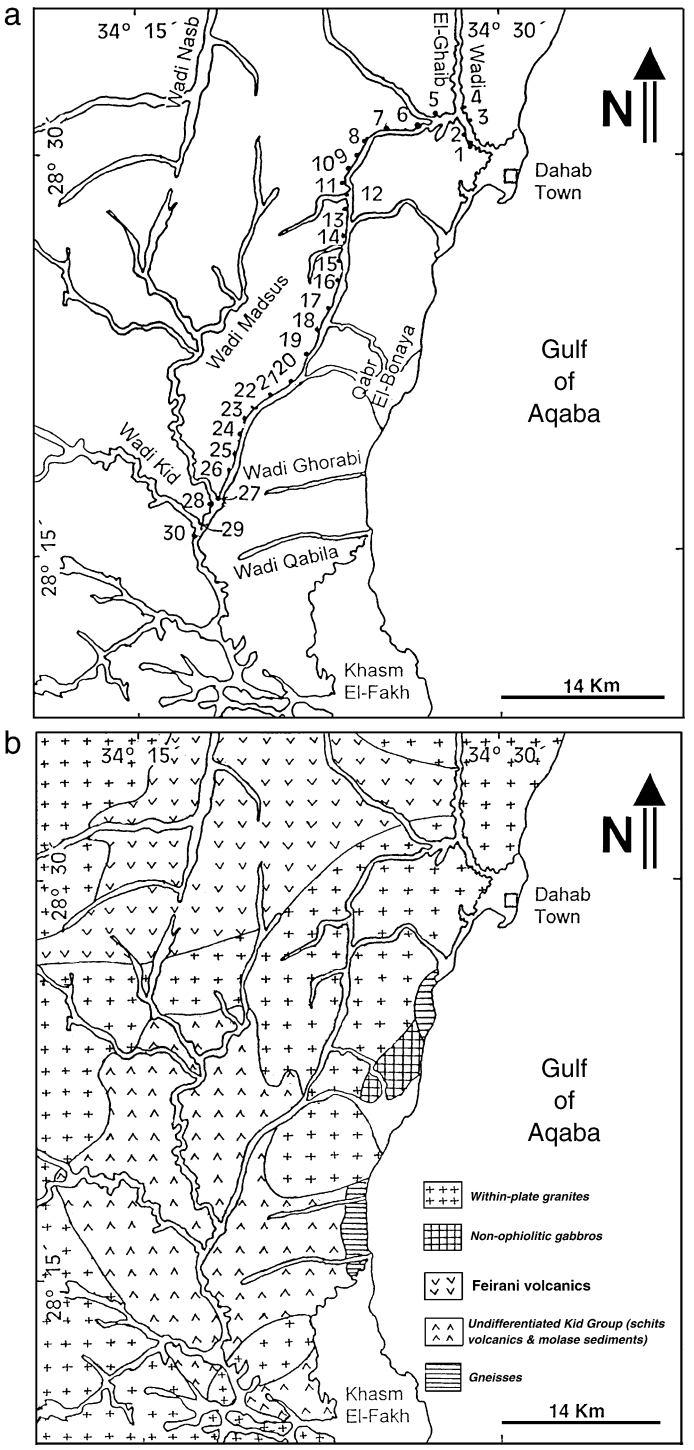

Fig. 2. (a) Sample locations and tributaries in the area west and south Dahab town. (b) Simplified geological map of Dahab area (compiled from El-Sheshtawy et al., 1988).

(1978) described two small outcrops of harzburgite and asbestos-bearing serpentinites to the south of Dahab town at Qabr El-Bonaya. Abdel Khalek et al. (1995) agreed with Shimron (1981) that these ultramafics represent part of a genuine ophiolite suite formed by back-arc spreading mechanism of an Andean-type crust. Some other workers, e.g. El-Gaby et al. (1987) and Takla and Hussein (1995), rejected the occurrence of any ophiolitic rocks in Sinai. These authors argued that the ultramafics of Dahab area are affiliated to the non-orogenic mafic–ultramafic association of Egypt.

To the west of Dahab town (at Gebel Feirani) and to the southwest (at Wadi Kid), thick metamorphosed and unmetamorphosed volcano-sedimentary successions are recorded (El-Metwally et al., 1999). Voluminous masses of granitic rocks occupy most of Dahab area (Fig. 2b). They are represented by both calc-alkaline and alkaline varieties formed at volcanic-arc and within-plate settings, respectively. Abundant post-granitic dykes and pegmatites dissect the Precambrian complex of Dahab–Nuweiba district (El-Sheshtawy et al., 1988; El-Metwally et al., 1999). The Oligo-Miocene rift of the Red Sea led to the injection of basaltic dyke swarms.

The sedimentary successions in the area of study are mainly represented by clastic sediments comprising sandstones and wadi deposits. The sandstones are either Cambrian or Cenomanian and they are adjacent to the Precambrian crystalline rocks along structural contacts, namely nonconformities and graben faults. On the other hand, wadi deposits are much younger in age and they range from Quaternary to Recent. They are stratigraphically discriminated into lacustrine and fluviatile deposits (wadi terraces), alluvial fans and loose sand. From the sedimentological point of view, the wadi terraces are unbraided stream sediments that result from the deposition of immature sediments carried by violent stream current during flood seasons. Usually, they range in thickness from 1.5 to 9 m and sometimes they show evidences of change in the current direction and power as indicated by the development of cross-bedding. Sediments of channel fillings at the middle of the stream course as well as the alluvial fans show some other primary sedimentary structures like graded-bedding. In general, the sediments of channel fillings at Dahab area are much more mineralogically immature than both the terraces and fans. All types of the investigated wadi deposits contain numerous pebbles, cobbles and boulders of granitic and volcanic rocks. For the present study, samples were only taken from the main wadi fillings (alluvial–colluvial sediments) at the junction between wadi tributaries and the course of the main stream.

3. Methodology

3.1. Sampling

Sampling was carried out in pits and channels on 30 outcrops representing the surveyed stations (Fig. 2a). Samples were essentially taken from the deposits at the depth of 30 to 50 cm from the wadi floor. Each sample was split into two parts, about 2.5 kg each. The first part was processed by gravimetric methods in order to concentrate heavy minerals including gold, whereas the second part was kept as a reserve for further separation and chemical analysis. Before splitting of the samples, large pebbles (>5 cm, average dimension) and cobbles were removed by hand in the field. Meanwhile, small pebbles (>2 cm) were rejected by manual sieving.

3.2. Analytical methods

The analytical work needed for the present study was achieved at the Central laboratories of the Geological Survey of Egypt in Cairo with the exception of XRD analysis that has been carried out using a Scintag machine housed at the Department of Geology, Cairo University. Major oxides were measured by wet chemistry. Both sodium and potassium oxides were determined by flame photometry whereas the rest of oxides were determined volumetrically. Analysis of trace elements was done by ICP-MS technique on a Philips spectrometer Model PW 8210 that works at 50 MHz. A series of standard samples (sandstones and granites) were used for the quantitative determination of trace elements. Each sample of the studied stream sediments as well as the standards were digested with $HCl/HClO_4$ (1:1) in Teflon bombs until incipient dryness. After digestion, the final residue was then dissolved in 2N HCl and diluted gravimetrically with distilled water to 100 ml. Gold content was determined by the fire assay technique on basis of 50

g silt-sized material. SEM-EDX microanalyses and microphotographs of some specific minerals were conducted on a Philips XL30 scanning electron microscope with energy dispersive X-ray attachment working at 30 kV acceleration voltage.

4. Mechanical analysis and mineral separation

4.1. Grain size analysis

Grain size analysis was performed at the Laboratory of Sedimentology at the Department of Geology, Cairo University. The analysis was carried out on three samples collected from each station (Fig. 2) making a total of 90 samples. Prior to heavy liquid and subsequent isodynamic separation, each sample was then discriminated into fractions using an automatic shaker using a phi set of standard sieves followed by sluicing and panning. Statistical grain size parameters were calculated according to the formulae given by Folk and Ward (1957). These parameters include mean grain size (MZ), inclusive standard deviation of sorting (σ_i), inclusive graphic skewness (Sk_i) and inclusive graphic kurtosis (K_G) as shown in Table 1. Grain size is distinctly variable, being represented by fine pebbles, granules and different categories of sands ranging from fine to very coarse sand. Coarse sand is the most frequent (43.3%) whereas the least frequent size is represented by equal values of fine pebbles and granules (3.3%). With respect to sorting, the inclusive graphic standard deviation values of Dahab stream sediments are indicative of poorly to very poorly sorted material (83.3 and 16.67, respectively). Scatter diagrams that correlates the mean grain size with the inclusive standard deviation can give good information about the environment in which the sediments are developed (Moiala and Weiser, 1968). Data of the Dahab stream sediments given in Fig. 3 show slight increase of sorting with the decrease of main grain size. Coarse and very coarse sand samples are clustered in the area of poor sorting on the scatter diagram. Very poorly and poorly sorted fractions are common, indicating that Dahab stream sediments are immature from the textural and mineralogical points of view although some samples show very slight tendency to be submature. This shows that transportation of debris was

Table 1
Range and average frequency distribution of some mechanical parameters of Dahab stream sediments

a) Graphic mean size

Total number of samples	Fine pebble		Granule		Very coarse sand		Coarse sand		Medium sand		Fine sand	
90	Number	%	Number	%	Number	%	Number	%	Number	%	Number	%
	3	3.3	3	3.3	39	43.33	36	40	6	6.67	6	6.67

b) Inclusive graphic standard deviation

Total number of samples	Very poorly sorted		Poorly sorted	
90	Number	%	Number	%
	15	16.67	75	83.3

c) Inclusive graphic skewness

Total number of samples	Coarse		Nearly symmetrical		Fine		Strongly fine	
90	Number	%	Number	%	Number	%	Number	%
	12	13.33	30	33.33	30	33.3	18	20

d) Inclusive graphic kurtosis

Total number of samples	Platykurtic		Mesokurtic		Leptokurtic		Very leptokurtic	
90	Number	%	Number	%	Number	%	Number	%
	18	20	45	50	24	26.67	3	3.33

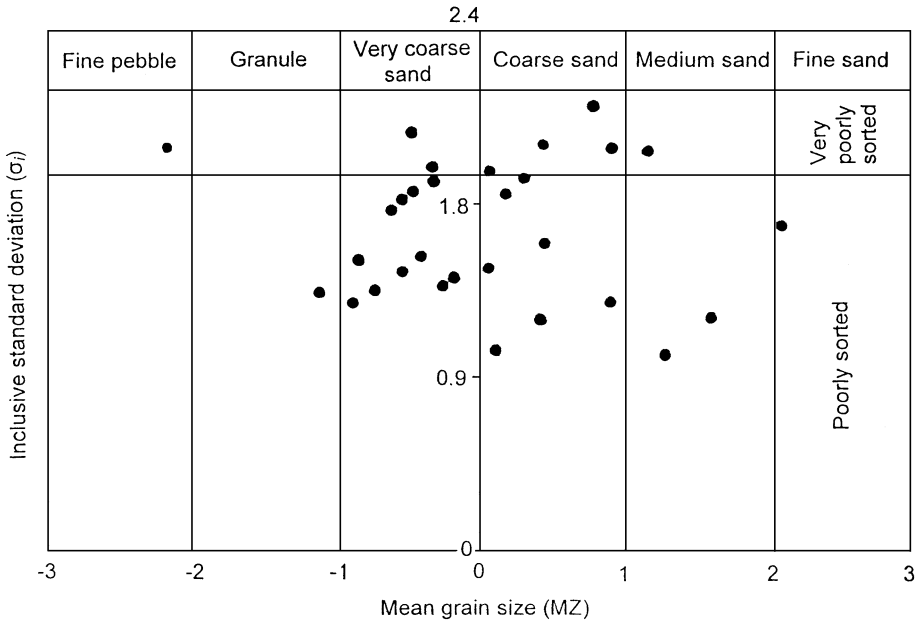

Fig. 3. Poor sorting of the studied sediments as indicated by the plot of MZ vs. σ_i.

negligible and the deposition took place in situ or close to the source. Such a conclusion is also supported by the grain morphology and the presence of unstable minerals and rock fragments. Morphologically, most of the investigated grains (>80%) are angular in shape and show little embayment.

4.2. Heavy liquid and isodynamic separation

Fractions of heavy minerals in the grain size ranges of 62–125 and 126–250 μm were mechanically separated from each investigated sample. After separation, by bromoform (specific gravity of 2.87), the index figure was calculated, which represents an expression of percentage of the heavy minerals in comparison to the light fraction components. For the purpose of detailed mineralogical investigation, the obtained heavy fractions were subjected to magnetic separation using a Frantz isodynamic separator.

Table 2 shows that the Dahab stream sediments are enriched in heavy minerals as indicated by their high index figure averaging 21.37% in the coarse size

Table 2
Range and average of heavy mineral frequencies[a] of Dahab stream sediments

Minerals and index figure	Grain size range: 126–250 μm			Grain size range: 62–125 μm		
	Minimum	Maximum	Average	Minimum	Maximum	Average
Index figure	1.8	38.22	21.37	7.92	60.9	25.94
Opaques	9.2	39.43	20.43	3.6	53.57	25.2
Biotite	6.18	69.55	22.23	4.93	66.99	35.7
Titanite	0.36	23.32	8.83	1.86	28.03	10.27
Hornblende	0.9	15.7	8.22	1.77	20.8	8.67
Epidote	0.9	24	7.9	0.17	11.88	2.89
Apatite	0.5	28.79	9.73	0	6.49	1.27
Monazite	0	9.36	1.63	0	5.84	0.89
Chlorite	0	2.64	0.39	0	4.58	0.78
Zircon	0.2	23.9	6.4	0	13.68	0.74

[a] Abundances of tourmaline and pyroxene are always close to nil.

Table 3a
Mineral composition of some light fractions and mud-cracks on basis of XRD analyses

Sample number and size range	Major constituents	Minor constituents	Trace constituents
26 (size: 62–125 μm)	quartz + albite	orthoclase + muscovite + biotite + microcline	Clinochlore + magnesio-hornblende + rutile
30 (size: 126–250 μm)	quartz + albite	orthoclase + muscovite + biotite	Clinochlore + magnesio-hornblende + anatase
30 (size: 62–125 μm)	quartz + albite	orthoclase + muscovite + biotite + microcline	Clinochlore + magnesio-hornblende + magnetite

range (126–250 μm) whereas it averages 25.94% in the fine size range (62–125 μm). Most of the investigated fractions were counted in both transmitted and reflected light after mounting in resin and polishing. The recorded nonopaque heavy minerals are arranged in decreasing order as follows: biotite-magnetite aggregates, monazite, apatite, titanite, zircon, zoisite, chlorite, amphiboles, pyroxenes, rutile and tourmaline.

4.3. Light fraction

Mineralogically, the light fractions of all samples contain abundant amounts of quartz, feldspars and micas (up to about 80%). This appears very reasonable because the hinterland is mostly granitic in composition. Table 3a shows that the major constituents of light minerals are quartz and albite. Lesser amounts of orthoclase, micas (muscovite and biotite) and microcline are also identified. It is evident that the trace constituents include both Mg-hornblende and clinochlore that suggests the incorporation of detritus derived from some mafic lithologies such as gabbros and basalts. Traces of some heavy minerals (rutile, anatase and magnetite) occur as overgrowths or inclusions commonly in quartz and less frequent in feldspars. Identification of amphibole and chlorite species was verified by X-ray diffraction (XRD).

It is possible to have a semiquantitative estimation of clay minerals percentages from their XRD data following the method of Pierce and Siegel (1969). A residue of floating clay minerals resulted from separation and centrifugal steps as well as a representative sample of mud-crack covers from station numbers 11 and 4, respectively, was chosen. It is evident that montmorillonite is the major constituent of the separated clay minerals amounting to 55% and 40% in these two samples, respectively (Table 3b).

Table 3b
Semiquantitative estimation of clay minerals percentages (according to the method of Pierce and Siegel, 1969)

Sample number	Montmorillonite	Illite	Kaolinite
4	40	30	30
11	55	15	30

5. Mineralogy and geochemistry

The following section gives a detailed mineralogical investigation of some economic minerals in the stream sediments of Dahab area. The mineralogical study was achieved using a normal optical microscope as well as a scanning electron microscope with an energy dispersive X-ray attachment (SEM-EDX). This gives information about the chemical composition of the investigated minerals. Also, some fractions of mineral concentrates were analysed by the ICP-MS technique in order to display their geochemical characteristics and their implication on genesis. Minerals are arranged here according to their abundances rather than their economic values.

5.1. Fe–Ti oxides and sulphides

Here, the Fe–Ti oxides and sulphides are lumped together because sulphides often occur as "nucleus-like" inclusions in these oxides, magnetite in particular (Fig. 4a). Sulphides are represented by fresh or goethitized pyrite and in rare cases chalcopyrite, pyrrhotite, galena and sphalerite. Some goethitized pyrite "nuclei" in magnetite also contain visible gold specks that are liberated upon the alteration of pyrite. All sulphide inclusions in the magnetite are auriferous and many of them also contain invisible gold in the structure. Rock fragments derived from silica stockworks contain abundant euhedral magnetite (Fig. 4b) whereas star-shaped and fish-bone magnetite is derived from quenched volcanic rocks (Fig. 4c and d).

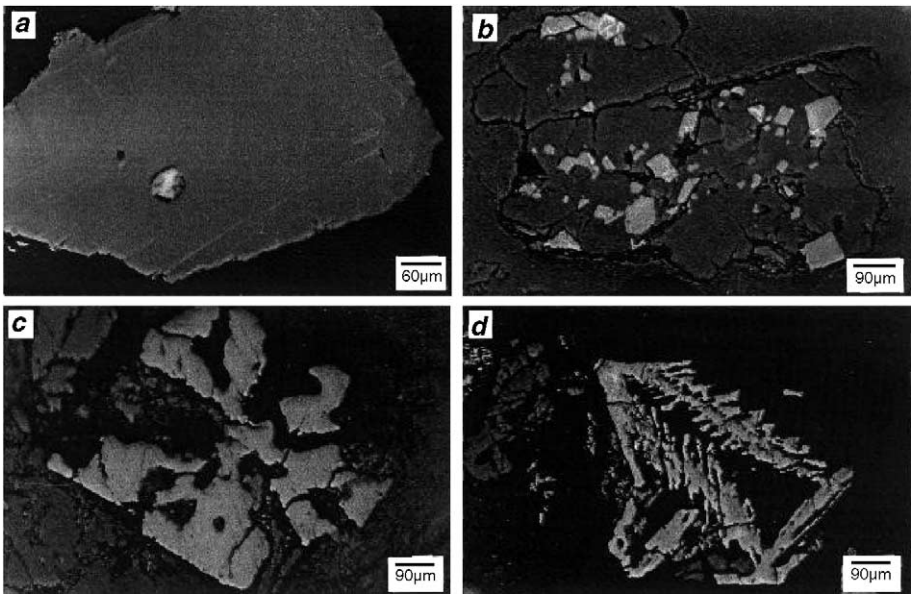

Fig. 4. Microphotographs of magnetite from Dahab stream sediments: (a) Ilmeno-magnetite grain containing fresh pyrite inclusion. (b) Quartz fragment containing euhedral magnetite octahedra. (c) Star-shaped magnetite. (d) Skeletal fish-bone magnetite.

Frequency distribution of the opaque minerals (Fe–Ti oxides, sulphides and their alterations) is presented in Table 4. It is clear that magnetite is the most predominant mineral among the concentrated opaque phases. Amount of homogeneous magnetite ranges from 48.57% to 78.11% with an average of 64.98% in the size range 126–250 μm, while it ranges from 60.03% to 75.22% with an average of 66.78% in the size range 62–125 μm. Hence, the range of homogeneous magnetite is wider in the coarse fraction. Much less frequencies of ilmenite–magnetite intergrowths are observed in both size fractions with the averages of 9.86% and 9.56%, respectively. Counted sulphide grains also include some few fine independent grains of silt size that are not enclosed by Fe–Ti oxides.

5.1.1. Textures and source of Fe–Ti oxides

Ore microscopic investigation of the magnetite revealed that it occurs as homogeneous magnetite with perfect octahedral cleavage (Fig. 5a). It appears that this magnetite is Ti-bearing as indicated by its pinkish tint. Extensive replacement of this magnetite by titanite indicates its titaniferous nature. In case of intergrown grains formed from solid solution, the optical properties of magnetite in the ilmeno-magnetite suggest a Ti-free or -poor composition, which is also supported by the absence of any replacement by titanite. The latter often contains exsolved lamellae of ilmenite along (111) and (001) planes, for example banded ilmeno-magnetite (Fig. 5b). The EDX microanalyses demonstrate that MnO content in exsolved ilmenite is markedly higher than in the homogeneous ilmenite amounting 10.92 and 1.78 wt.%, respectively (Table 5). This suggests that Mn^{2+} is concentrated in the exsolved ilmenite upon cooling of ilmeno-magnetite solid solution in the magmatic conditions. In many cases, the homogeneous ilmenite exhibits typical patchy rutile–hematite alteration (Fig. 5c). Also, ilmenite in the studied sediments host exsolved hematite blebs forming hemo-ilmenite grains. In addition to the banded intergrowth, ilmeno-magnetite grains display other types of exsolution textures, namely fine network, coarse-trellis, sandwich, composite, internal and external granules.

5.1.2. Geochemical behaviour

The chemical analysis of the concentrated Fe–Ti oxides by the ICP-MS technique (Table 6) shows appreciable contents of Zn, Pb and As up to 29, 36

Table 4
Frequency distribution of opaque minerals separated as two independent fractions

Mineral	Magnetite		Ilmenite		Goethite and rutile	Sulphides
Station number	Homogeneous	Intergrowth	Homogeneous	Intergrowth		
Size range: 126–250 μm						
1	63.23	7.00	13.13	9.41	3.72	3.50
3	53.71	12.62	13.63	8.10	6.61	1.00
5	70.60	12.97	8.10	6.30	1.39	0.69
7	59.66	10.42	10.42	3.95	0.85	2.56
10	63.52	10.82	13.18	4.39	3.70	4.40
12	71.60	5.78	16.27	3.11	1.18	2.07
16	70.40	5.40	9.48	8.31	2.90	3.50
20	67.83	11.90	2.97	10.56	4.32	2.43
21	78.11	10.62	3.70	1.29	1.45	4.83
26	48.57	10.80	12.70	16.83	10.48	0.63
28	63.08	8.19	15.57	7.98	2.99	2.20
29	69.42	11.85	10.20	4.96	2.75	0.83
Average	64.98	9.86	11.74	6.10	3.53	2.39
Size range: 62–125 μm						
1	68.49	10.98	12.73	4.62	1.87	1.30
3	62.05	11.69	13.56	8.08	2.45	2.16
5	75.22	9.86	8.90	3.37	1.32	1.32
7	57.08	10.15	24.43	5.50	1.42	1.42
10	62.02	9.52	20.82	4.48	0.59	2.20
12	73.71	2.52	19.86	1.40	0.56	1.96
20	71.71	10.63	4.34	5.00	4.02	4.34
21	70.87	9.85	9.71	3.04	2.75	3.77
26	66.62	11.17	13.65	3.48	3.85	1.24
28	60.03	9.21	21.94	3.65	2.14	2.02
Average	66.78	9.56	14.99	4.26	2.10	2.17

and 27 ppm, respectively. Abundances of these trace elements are attributed to the presence of sulphide inclusions in the magnetite, which is consistent with the ore microscopic investigation. Based on the data of Table 6, bulk composition of the Fe–Ti oxide concentrates indicates an inverse relationship between TiO_2 and FeO (Fig. 6a). Nb content is appreciable (13–23 ppm), which is in turn positively correlated with Zn and As (Fig. 6b and c). On the other hand, Ta content is lower (2–3 ppm) and exhibits no correlation with Nb (Fig. 6d).

5.2. Zircon and other radioactive minerals

The stream sediments of Dahab area contain considerable amounts of zircon. Some separated fractions of heavy minerals contain zircon up to 23.90% and 13.68% in the size ranges of 126–250 and 62–125 μm, respectively (Table 2).

5.2.1. Zircon morphology, radioactivity and source

Zircon mostly occurs either as short or long prismatic crystals with bipyramidal terminations. Short zircon grains are sometimes zoned and twinned. It is colourless and charged with very fine inclusions of earlier generation of zircon in addition to thoeite, apatite and opaques. Short zircon displays evidence of metamictization such as cracking (Fig. 5d) due to the presence of radioactive atoms in the crystal structure that is also documented by the chemical data of the present work. Radioactive nature of the studied zircon is also manifested by its pleochroic haloes in biotite. On the other hand, long zircon grains are yellow in colour, stained by Fe oxides and commonly zoned. Short and long zircon grains are derived from volcanic-arc granitoids and within-plate granites of Egypt, respectively (Kabesh et al., 1976; El-Sheshtawy and Abu El-Leil, 1989; Eliwa et al., 2000). Dawoud (1995) attributed the colouration of zircon

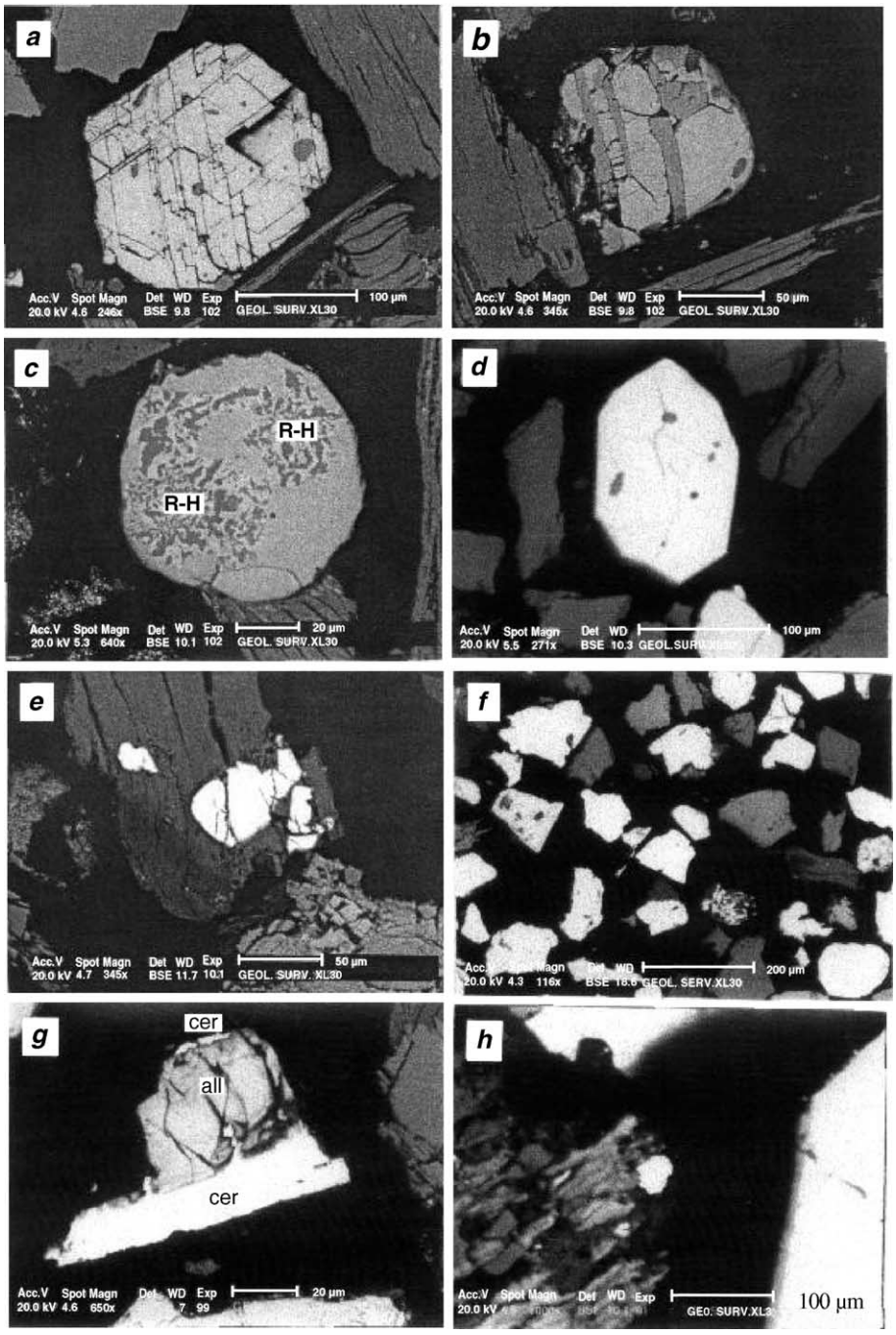

Fig. 5. BSE images of heavy minerals by the scanning electron microscope: (a) Homogeneous magnetite exhibiting perfect octahedral (111) cleavage. (b) Banded ilmenite (*dark*)-magnetite (*light*) exsolution intergrowth. (c) Rounded homogeneous ilmenite showing alteration to rutile–hematite (R–H) mixture. (d) Cracking and inclusions in metamict zircon. (e) Thorite (*light*) inclusions in biotite. (f) Bright monazite grains. (g) La-cerianite (cer) invading and rimming allanite (all). (h) Native silver grain in association with chloritized biotite.

Table 5
Spectral EDX microanalyses of some heavy minerals

Oxides	Ilmenite (wt. %)		Oxides	Thorite (wt. %)	
	Homogeneous	Exsolved			
TiO_2	48.14	50.13	SiO_2	9.48	20.87
MnO	1.78	10.92	P_2O_5	7.60	4.48
Fe_2O_3	50.08	38.95	CaO	2.57	1.73
Total	100.00	100.00	V_2O_5	6.45	0.00
			Ce_2O_3	4.82	0.00
			ThO_2	69.07	72.93
			Total	100.00	100.00

REE-bearing minerals

Element	Monazite (wt.%)	Cerianite (wt.%)	Oxides	Allanite (wt.%)
Ce	38.60	59.17	SiO_2	38.02
La	20.75	34.56	TiO_2	2.99
Ca	0.75	6.27	Al_2O_3	12.20
Si	1.53	0.00	MgO	1.11
P	19.42	0.00	CaO	12.96
Ag	5.45	0.00	Fe_2O_3	17.87
Nd	11.10	0.00	Ce_2O_3	14.83
Sm	1.58	0.00	Total	100.00
Gd	0.81	0.00		
Total	100.00	100.00		

in the Egyptian granitic rocks to hydrothermal solutions of exotic origin. However, the role of some elements such as Y, Th and U should not be excluded when the question of zircon colouration is taken into consideration.

5.2.2. Chemistry of zircon

The chemical composition of the analysed zircon concentrates is given in Table 7. Fig. 7a shows positive correlation between HfO_2 and ZrO_2. The HfO_2/ZrO_2 ratio in zircon ranges from 0.009 to 0.015. Hf tends to replace Zr especially along the crystal peripheries during hydrothermal activity (Correia-Neves et al., 1974). HfO_2/ZrO_2 ratio in the range of 0.013–0.019 is very characteristic of zircon from fresh granites. The HfO_2 content in the analysed zircon ranges from 0.53 to 0.9 wt.%. The common range of HfO_2 in most of naturally occurring zircon is 0.6–3.0 wt.%. Average HfO_2 content of detrital zircon in sandstones amounts to 1.3 wt.% (Owens, 1987).

ThO_2 and UO_2 are positively correlated (Fig. 7b) indicating that the enrichment of radioactive elements in the granitic source was controlled by normal magmatic differentiation. Two discriminative fields of U-poor and U-rich zircons are shown in Fig. 7c. Two analyses of zircon show high contents of ThO_2 (2.24 and 2.35 wt.%). El-Kammar (personal communication) attributes high contents of Th in some Egyptian zircon to the presence of very fine inclusions of uranothorite. On the other hand, Gindy (1961) concluded that Th content in zircon is most probably related to the presence of Th in the zircon structure and discarded any correlation with the presence of radioactive inclusions.

Thorite, usually as inclusions in biotite, was also identified in Dahab stream sediments (Fig. 5e). ThO_2 content of thorite reaches up to 72.93 wt.%. It is evident that both Th and Si are partly substituted by V and Ce. Upon such substitution, ThO_2 decreases to 69.07 wt.%. SiO_2 is greatly variable from 20.87 to 9.48 wt.% (Table 5).

5.3. REE-bearing minerals

It was difficult to identify some very fine minerals using the normal optical microscope. Identification was possible using a scanning electron microscope (SEM) with an EDX microanalyser attachment. In the studied samples of Dahab stream sediments, monazite contains about 70 wt.% rare-earth elements, namely 11.1 wt.% Nd, 38.6 wt.% Ce and 20.75 wt.% La (Fig.

Table 6
Bulk composition of Fe–Ti oxides concentrated from Dahab stream sediments (size range: 62–250 μm)

Oxide wt.%	Station number				
	11	12	18	23	29
SiO_2	0.42	0.53	0.39	0.45	0.50
TiO_2	40.58	39.37	38.65	38.61	39.53
Al_2O_3	0.28	0.36	0.60	0.47	0.52
Fe_2O_3	14.35	15.11	15.73	15.47	14.81
FeO	42.46	42.60	43.06	42.93	42.81
MnO	0.55	0.48	0.61	0.67	0.59
MgO	0.51	0.53	0.48	0.52	0.50
CaO	0.71	0.81	0.68	0.79	0.61
Total	99.86	99.79	100.20	99.91	99.97
Trace elements (ppm)					
Ta	3	2	3	3	2
Nb	15	20	13	18	23
Zn	19	23	25	20	29
Cu	3	5	4	3	2
Pb	20	36	31	29	34
As	16	22	19	20	27

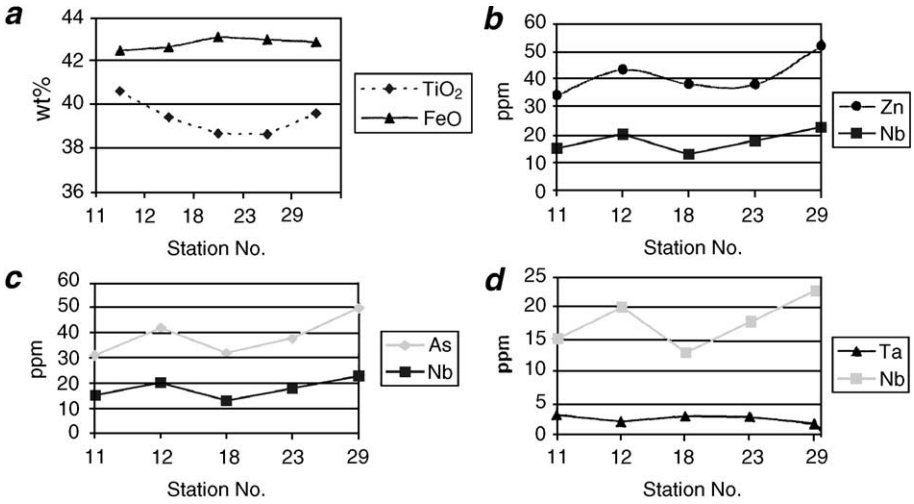

Fig. 6. Binary geochemical relations of Fe–Ti oxides: (a) Negative correlation between FeO and TiO_2. (b) Positive correlation between Nb and Zn. (c) Positive correlation between Nb and As. (d) Indefinite correlation between Nb and Ta.

5f and Table 5). Cerianite (Ce-oxide mineral) is also present where Ce amounts to 57.17 wt.% and contains 34.56 wt.% La (Fig. 5g and Table 5). Enrichment of cerianite in La classifies it as La-rich variety. Also, the latter figure shows that the recorded La-cerianite invades allanite, i.e. the former postdates the latter. Spectral analysis of allanite revealed that it is free of La but Ce-bearing (Table 5).

5.4. Precious metals

One of the main targets of the present study is the detection and evaluation of precious metals, especially gold, in the stream sediments of Dahab area.

5.4.1. Occurrence and detection of native gold

This section presents special emphasis on gold because several particles of native gold were detected during the early phases of the present work alongside with the microscopic investigation. Gold was checked and analysed by the scanning electron microscope (SEM) with an EDX and the concentration of gold was determined by the technique of fire assay just for preliminary estimation, which of course still needs more detailed studies regarding its economic potentiality and the recommended method of extraction. Based on the microscopic study, there are two modes for gold occurrence in Dahab stream sediments. The first form is represented by free dispersed gold. The

Table 7
Chemical composition of zircon from Dahab stream sediments (size range: 62–250 μm)

Zircon type	U-poor												U-rich		
Oxide wt.%	Station number														
	1	5	6	7	8	9	17	20	21	22	25	27	4	13	24
SiO_2	31.42	33.46	31.68	32.29	35.64	35.00	32.28	29.66	31.49	34.19	33.50	36.09	28.19	29.20	31.08
ZrO_2	62.51	59.83	59.51	63.75	57.31	60.53	60.81	60.39	63.49	62.05	62.65	58.92	58.21	57.17	58.11
HfO_2	0.82	0.78	0.69	0.83	0.74	0.84	0.90	0.69	0.83	0.69	0.72	0.53	0.81	0.79	0.66
Fe_2O_3	1.35	2.08	3.25	0.05	1.12	1.55	1.96	3.25	0.05	0.12	0.00	1.15	3.68	3.70	2.25
ThO_2	0.01	0.03	0.05	0.08	0.02	0.03	0.08	0.07	0.10	0.10	0.19	0.01	2.35	2.24	2.10
UO_2	0.04	0.05	0.15	0.09	0.04	0.04	0.11	1.19	0.88	0.10	1.19	0.05	3.68	3.67	3.05
Total[a]	96.15	96.23	95.33	97.09	94.87	97.99	96.14	95.25	96.84	97.25	98.25	96.75	96.96	96.77	97.25

[a] Low total of some analyses is attributed the presence of Fe_2O_3 and SnO in the range of 0–3.70 and 0.09–3.25 wt.%, respectively. Traces of REE and rare metals are also present especially Y and Ta up to 700 and 207 ppm, respectively.

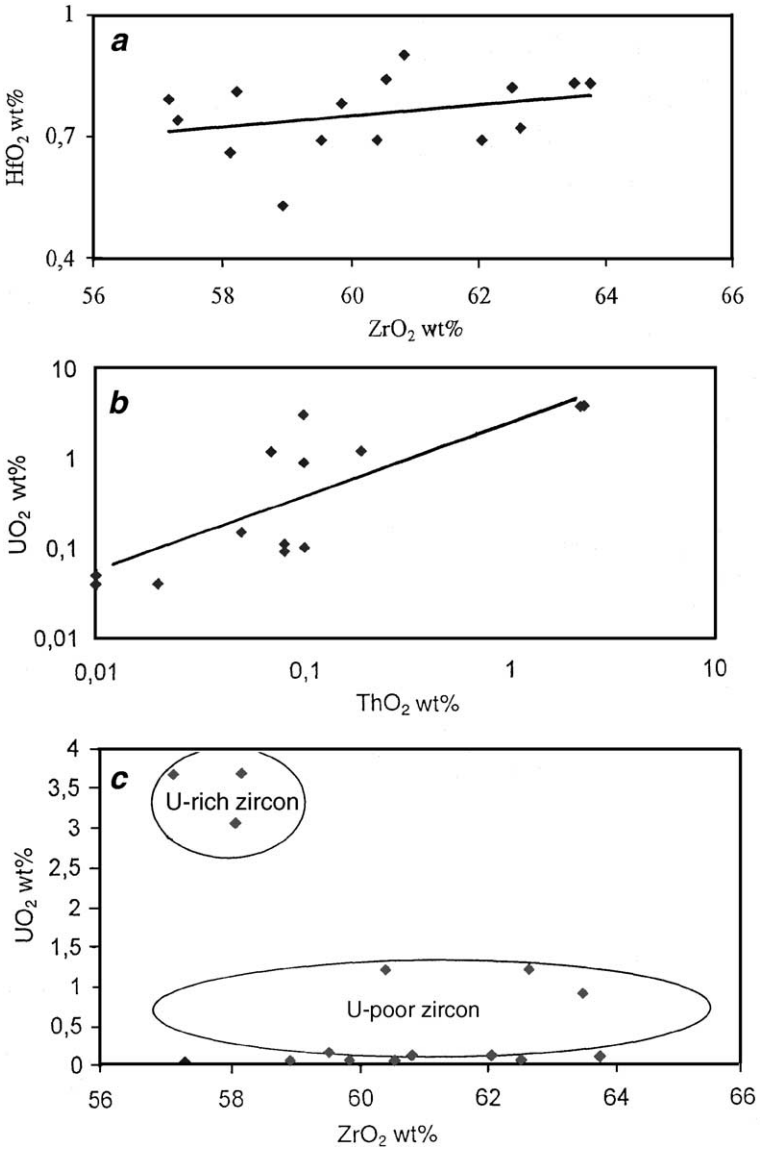

Fig. 7. Binary geochemical relations of zircon: (a) Positive correlation between ZrO_2 and HfO_2. (b) Positive correlation between ThO_2 and UO_2. (c) Discrimination of zircon into U-poor and U-rich varieties.

second mode shows the occurrence of gold as inclusions in some silicates, for example quartz, titanite and amphiboles in addition to magnetite, pseudobrookite and sulphides. Independent gold grains, and possibly invisible gold, often associate sulphide inclusions in magnetite rather than ilmenite.

SEM images suggest that gold is concentrated in the silt fraction (40–62 μm). Also, extremely fine "dusty" gold (≤ 40 μm) was identified in most stations as free gold. SEM images show that free gold grains still retain some of its cubic faces (Fig. 8a) whereas it is skeletal and occurs as leaf-like inclusion in oxyhornblende for instance (Fig. 8b). Occurrence of gold in oxyhornblende suggests that it could be possibly derived from unmetamorphosed gabbroic rocks. This type of Ti-rich gabbro occurs as small

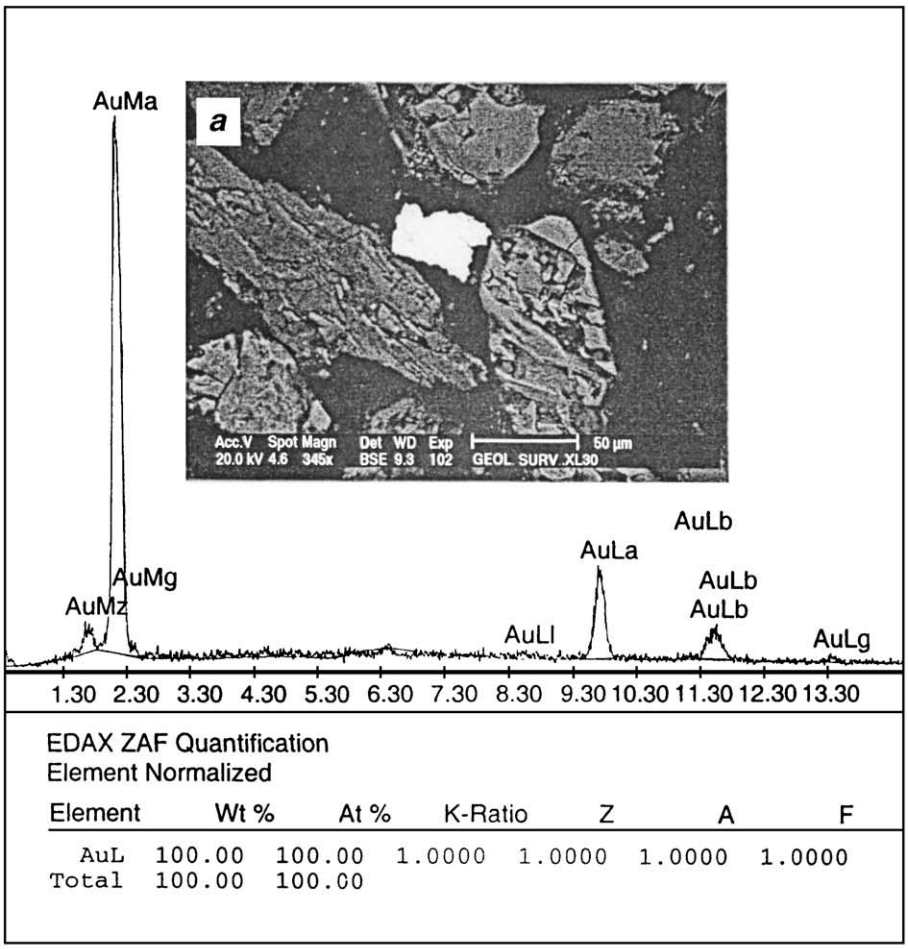

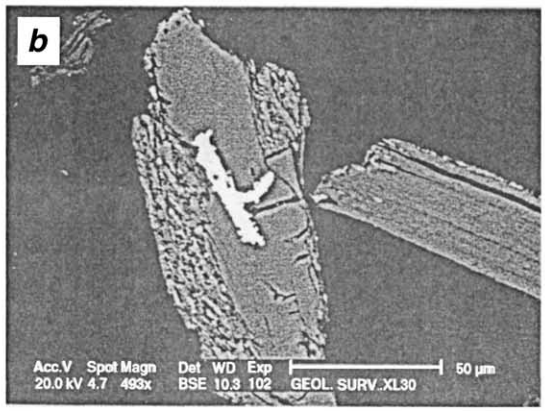

Fig. 8. Gold in the studied stream sediments: (a) Free gold grain and its EDX spectra. (b) Leaf-like gold inclusion in oxyhornblende.

Table 8
Background concentration of gold in the Precambrian source rocks at Dahab area

Rock type	Au (ppm)	Number of analysed samples
Data of the present study		
Diorite-granodiorite	0.1–0.5	3
Pink granite	0.3–0.6	3
Feirani rhyolite[a]	0.3–0.5	2
Data cited in Khaled and Oweiss (1995b)		
Quartz veins	0.3–0.6	100
Alteration zones	0.3–16.5	150
Kid rhyolite sheets[a]	0.6–0.8	unknown

[a] Sulphide-bearing rhyolites.

masses to the north of Dahab area (Surour and Kabesh, 1997). According to these authors, it is typical nonophiolitic gabbro with clear alkaline tendency.

5.4.2. Gold content

Most workers believe that Sinai is not a province for gold mineralization in Egypt in comparison to the Eastern Desert. Generally, background concentration of gold in the source rocks (the Precambrian basement) is low and no major zones of mineralization in Sinai could be traced. In some local areas, gold occurs as small-tonnage dispersed grains, as well as invisible gold inside the sulphides in the quartz veins along local shear planes at Wadi Kid. Table 8 shows that gold background in the volcanics and granitic rocks never exceeds 0.8 ppm. At Wadi Kid, gold in some altered rocks is exceptionally high, reaching up to 16.5 ppm (Khalid and Oweiss, 1995b). These authors also added that formation of "listwanite" upon carbonatization of the ultramafic rocks was capable to enrich gold in this altered variety to 0.8 g/t. It appears that gold content in the narrow quartz veins (7–25-cm wide) is close to that of both volcanics and granitic rocks in the range of 0.1–0.8 ppm. So, it is evident that placer gold in the stream sediments is the only potential source of the precious metal in Sinai. Relief and mechanical weathering are the main controlling factors in the development of this type of arid environment placers.

In order to have an accurate estimation of gold concentration in the silt-sized fractions (size ≤ 40 μm and even up to 62 μm), samples taken from different wadi tributaries at Dahab area were subjected to fire assay measurements. This method is accurate and convenient because the result is based on the actual amount of gold in the sample on basis of metal extraction on the laboratory scale. The obtained data of fire assay (Table 9) show that highest gold content is recorded at Wadi Qabila (15.34 g/t). On the other hand, averages of gold range from 1.3 to 3.01 g/t for the following Wadis: Kid, Um Alaqa, Qenai, Abu Khisheib, Um Shoki and Dahab. From the economic point of view, gold is workable in most of the investigated tributaries because the lowest range value is 1.3 g/t. Extraction of gold attaining such concentrations can encourage investment of mining at Dahab area. Some productive gold prospects of stream sediments containing Au around 1.0 g/t are known from other places worldwide, for example in Saudi Arabia, which is the closest example to Sinai. Mining and extraction of gold from loose sediments containing free gold is inexpensive.

5.4.3. Native silver

Similar to gold, microscopic investigation indicates the presence of few silver grains. Also, some bulk ICP-MS analyses for Ag was done. Again, the metal estimation is not accurate by such method where it gives Ag in the range of 0.22–0.70 ppb. Irregular subrounded nature of the recorded native silver can be seen in a SEM image (Fig. 5h). Amount of silver grains decreases in the gold-rich samples, which is

Table 9
Gold content as determined by fire assay of the silt fraction (<40 μm)[a]

Locality (name of tributary)	Gold content (g/t)	
	Range	Average
Wadi Um Misma	0.10–0.70	0.40
Wadi Dahab	1.40–2.60	1.50
Wadi Um Shoki	1.26–2.40	1.83
Wadi Abu Khisheib	1.84–2.16	2.00
Wadi Qenai El-Rayan	1.90–3.18	2.54
Wadi Um Alaqa	1.60–4.00	2.80
Wadi Madsus	0–1.20	0.6
Wadi Kid	1.50–4.52	3.01
Wadi Qabila		15.34

[a] Number of analysed samples in all is five except for Wadi Qabila (one sample).

attributed to differential transportation and weathering (Vavelidis et al., 1997).

6. Fe–Ti oxides as indicators of provenance

With respect to their provenance, the textural fabrics of Fe–Ti oxides give useful clues about their source. Usually, the detrital Fe–Ti oxides that are derived from plutonic igneous source display exsolution textures more frequently than those originated from metamorphic rocks (Darby and Tasng, 1987; Basu and Molinaroli, 1989, 1991). In general, igneous rocks cool faster and quench at higher temperatures than metamorphic rocks. Some samples of Dahab stream sediments contain homogenous magnetite derived from quenched volcanic rocks, being represented by typical skeletal magnetite such as fish-bone, cruciform and star-shaped as previously shown in Fig. 4. Lack of roundness in the majority of homogeneous ilmenite indicates that they are derived from a proximal source. Probable source of this ilmenite is the gabbroic rocks some 100 km away from Dahab town. On the contrary, euhedrality of magnetite and its chemistry suggest that it is derived from the voluminous granitic rocks. Surour and Kabesh (1997) discriminated the granitic rocks of north Dahab area at Wadi Risasa on basis of Fe–Ti oxide textures. They (op. cit.) characterized the volcanic-arc granitoids by the presence of exsolved ilmeno-magnetite, hemo-ilmenite and homogeneous magnetite with sulphide "nuclei", while no exsolution fabrics are recorded in the within-plate granites that contain much abundant homogeneous magnetite and ilmenite.

Alteration and replacement of Fe–Ti oxides in Dahab stream sediments comprise pre- and postdepositional textural fabrics. Predepositional textures include normal and heat martitization of magnetite, alteration of both magnetite and ilmenite to titanite especially in grains of metamorphic origin and finally the metamorphic alteration of ilmenite to rutile–hematite. The observed postdepositional textures may also include martitization of magnetite, but they are basically represented by the formation of microcrystalline and colloform goethite–"limonite". There is an agreement that alteration of detrital Fe–Ti oxides takes place through dissolution and degree of alteration is more pervasive for magnetite than for ilmenite (Morad and Aldahan, 1986). Alteration process is linked to both cation mobility and conditions of oxidation.

7. Discussion and interpretations

Field and laboratory work of the present study reveals that Dahab stream sediments can be considered as a potential source of gold. Some other minerals such as Fe–Ti oxides, zircon and REE-bearing minerals can be also exploited as by-products. Mineralogical and geochemical studies were carried out on separated heavy mineral fractions in the size range of 126–260 and 62–125 μm. Magnetite is the predominant Fe–Ti oxide in Dahab stream sediments. Homogenous magnetite often encloses "nucleus-like" inclusions of sulphides (mostly pyrite). Several types of ilmeno-magnetite exsolution intergrowths have been recorded. It is evident that Mn^{2+} is concentrated in exsolved ilmenite lamellae when the original titanomagnetite solid solution is cooled in magmatic conditions. MnO content in ilmenite exsolved in magnetite is much greater than in homogenous ilmenite amounting to 10.92 and 1.78 wt.%, respectively. Two representative samples of Dahab stream sediments were selected in order to evaluate the economic potentiality of the studied sediments in terms of Fe–Ti ore abundance. These samples were collected from Wadi Abu Khisheib and Wadi Um Misma because the values of index figure in both suggest remarkable enrichment of opaque minerals. Weight of investigated raw samples (i.e. prior to any type of separation) is about 6 kg each. Grain size was ≤ 1 mm after hand picking of coarse pebbles. Data of mineral recovery of these raw samples show that the studied sediments can yield up to 15.12% magnetic minerals, mostly magnetite. Also, each sample was subjected to isodynamic separation at variable strength of magnetic field. The data presented in Table 10 give the details of recovery of magnetic minerals from the studied samples. These samples are considered as technological samples that can also give an approximate estimation of zircon and monazite content, usually >10% of the raw materials. Technological samples are the laboratory-scale equivalents to their industrial counterparts.

Zircon displays distinct variation in colour, morphology, chemistry and provenance. It is concluded

Table 10
Recovery of magnetic minerals from Dahab stream sediments

Size of fraction: 0.5–1.0 mm	Size of fraction: <0.5 mm
I. Raw sample of wadi deposits (size < 1.0 mm); weight: 6.10 kg; sample location: Wadi Abu Khisheib	
Mag.[a] I: 50.6 g	Mag. I[b]: 187.2 g
Mag. II: 70.7 g	Mag. II[b]: 131.7 g
	Mag. III[b]: 101.1 g
Zircon + monazite: 62.7 g	Zircon + monazite: 76.5 g
Total heavy minerals: 184 g	Total heavy minerals: 496.5 g
Total magnetic minerals: 121.3 g	Total magnetic minerals: 420 g
Total amount of magnetic minerals with respect to total heavies: 79.45%	
Total amount of magnetic minerals in the raw sample: 8.87%	
II. Raw sample of wadi deposits (size < 1.0 mm); weight: 6.26 kg; sample location: Wadi Um Misma	
Mag. I: 116.2 g	Mag. I: 260.2 g
Mag. II: 85.9 g	Mag. II: 332.3 g
	Mag. III: 150.2 g
Total amount of magnetic minerals in the raw sample: 15.12%	

Examples from two distant stream tributaries.

[a] Mag. refers to total magnetic minerals (99% Fe–Ti oxides, mostly magnetite followed by ilmenite and hematite).

[b] Mag. I, II and III refer to magnetite resulted from isodynamic separation at 500, 1000 and 1400 G, respectively.

that zircon in the studied stream sediments is derived from different granitic sources, namely volcanic-arc granitoids and within-plate granites. It was also possible to discriminate between U-poor and U-rich varieties of zircon containing UO_2 in the ranges of 0.04–1.19 and 3.05–3.68 wt.%, respectively. Radioactivity of U-rich zircon is attributed either to the presence of thorite and uranothorite inclusions or to partial replacement of zirconium by uranium and thorium in its tetragonal lattice. In addition to zircon, Dahab stream sediments contain other radioactive minerals such as thorite that contains traces of both V and Ce. Thorite and REE-bearing minerals (monazite, allanite and La-cerianite) occur in most cases as inclusions in biotite. Confinement of these minerals to biotite indicates their derivation from granitic rocks, granites and pegmatites. Noticeable enrichment of any stream sediments in high field-strength elements (HFSE) especially U, Zr, Th, Hf and REEs is a strong indication of granitic pegmatite source rocks (Chandrajiath et al., 2001). Pegmatites invading granites are commonly distributed in the Precambrian rocks of Dahab area.

Detailed mineralogy of Dahab stream sediments indicates the presence of precious metals, namely native gold and silver. It seems that topography has its important role in the development of such placers. Narrow gullies and valleys dissecting the uplifted Precambrian basement complex manifest the development and preservation of Dahab placers. Levson and Blyth (2001) reached similar conclusion but on fluvial gold placers in northwest British Columbia. The fire assay data suggest that placer gold in the studied sediments, mostly proximal to the upstream, sometimes reaches 15.34 g/t. The lowest average of gold content in the investigated tributaries amounts to 1.3 g/t. Such values suggest that the metal is workable from the economic point of view since extraction of free native gold from loose sediments is greatly profitable. Search for gold in the downstream outside the area of study (e.g. Khashm El-Fakh coastal fan) will probably yield much more concentrations. Jennex et al. (2000) explained that exhumation of gold in paleoplacers is a function of hydraulic processes that lead to sorting and accumulation of heavy minerals. Construction of motels and hotels at Dahab town made the search for gold in the downstream sediments very difficult. Dahab is considered as the most attractive resort for diving on the Gulf of Aqaba.

No evidence for gold mining in Sinai is found in both geological and archaeological literature although the name Dahab in Arabic means "gold". Thus, research into the historical background of gold in Sinai can be an interesting point of future archaeological study especially when it is focused on the Islamic period. Some workers presented data on the exploitation of gold during the Islamic rule in southern Israel at Wadi Tawahin close to Elat resort (Gilat et al., 1993). On basis of ^{14}C dating of pottery at this site, these authors calibrated an age of 970 AD, which is equivalent to the Early Islamic period. The Arabs might extend their activities for gold mining to Sinai, which of course needs rigid archaeological documentation. Similar to the discovery of gold in Dahab stream sediments by the present authors, Bogoch et al. (1990, 1993) discovered a gold anomaly at Nahal Roded area in southern Israel. In this respect, large-scale field and laboratory detailed studies for mineral exploration of placer gold in Sinai is strongly recommended. Basin analysis and statistical data processing of gold in the sediments of wadi terraces and alluvial

fans should be carried out (Petkovic and Babovic, 1995) for accurate evaluation of reserves.

8. Conclusions

It is evident that type and abundance of heavy minerals in Dahab area can be linked to general source rocks. Textural immaturity of the investigated sediments indicates negligible transportation in this arid environment. Mineralogical aspects and chemistry of Fe–Ti oxides and zircon suggest derivation from both volcanic-arc and within-plate granites. It is also concluded here that dispersion of gold in the placers of arid environments can be of multiple sources. Dispersion pattern of gold is controlled by the metal background concentration in the source rocks, in addition to relief and distance of transportation. Placer gold in this case is concentrated in the silt-sized fraction ($\leq 40-63$ μm) by winnowing of fine sediments. It is recommended that exploration of gold in arid regions must be directed essentially to the silt-sized fraction. In few cases, coarse gold ≥ 63 μm is derived from the mechanical weathering of pegmatites.

Acknowledgements

The authors are greatly indebted to Dr. D. Craw and other anonymous reviewers for their constructive comments and improvement of the manuscript. The authors are grateful to Mr. Abdel Monem Hussein for carrying out the fire assay analysis of gold, and to Prof. Emil Makovicky (Copenhagen University, Denmark) for his comments and improving the language.

References

Abdel Khalek, M.L., Abdel Maksoud, M.A., Abdel Tawab, M.A., El-Bedawi, M.A., 1995. An ophiolite mélange complex south of Dahab, Sinai, Egypt. Ann. Geol. Surv. Egypt 20, 1–18.

Basu, A., Molinaroli, E., 1989. Provenance characteristics of detrital opaque Fe–Ti oxide minerals. J. Sediment. Petrol. 59, 922–934.

Basu, A., Molinaroli, E., 1991. Reliability and application of detrital opaque Fe–Ti oxide minerals in provenance determination. In: Morton, A.C., Todd, S.P., Haughton, P.D.W. (Eds.), Developments in Sedimentary Provenance Studies. British Geol. Surv., Keyworth, U.K., Geol. Soc. Special Publ., vol. 57, pp. 55–65.

Beyth, M., Hrunhagen, H., Zilberfarb, A., 1978. An ultramafic rock in the Precambrian of eastern Sinai. Geol. Mag. 115, 373–378.

Bogoch, R., Beyth, M., Shirav, M., Halicz, L., 1990. Geochemistry of ephemeral stream sediments in the Precambrian terrain of southern Israel. Israel Geol. Surv. (Report GSI/35/90, 97 pp.).

Bogoch, R., Shirav, M., Beyth, M., Halicz, L., 1993. Geochemistry of epehemeral stream sediments in the Precambrian mountainous arid terrain of southern Israel. J. Geochem. Explor. 46, 349–364.

Chandrajiath, R., Dissanayake, C.B., Tobschall, H.J., 2001. Enrichment of high field strength elements in stream sediments of a granulite terrain in Sri Lanka—evidence for a mineralized belt. Chem. Geol. 175, 259–271.

Correia-Neves, J.M., Lopes-Nunes, J.E., Sahama, T.G., 1974. High hafnium member of the zircon-hafnon series from the granite pegmatites of Zambezia, Mozambique. Contrib. Mineral. Petrol. 48, 73–80.

Darby, D.A., Tasng, Y.W., 1987. Variation in ilmenite composition within and among drainage basins: implications for provenance. J. Sediment. Petrol. 57, 831–838.

Dawoud, M., 1995. Petrography, geochemistry and tectonic environment of the granitic rocks of Gabal Abu El Hassan-Gabal Abu Samuk, North Eastern Desert, Egypt. PhD Thesis. Fac. Sci., Menoufia Univ. Egypt.

El-Gaby, S., List, F.K., Tehrani, R., 1987. Geology, evolution and metallogenesis of the Pan-African belt in Egypt. In: El-Gaby, S., Greiling, O. (Eds.), The Pan-African of Northeast Africa and Adjacent Areas. Fieder. Vieweg und Sohn, Braunschweig-Wiesbaden, Germany, pp. 17–68.

Eliwa, H.A., Dawoud, M., Negendank, J.F.W., 2000. Morphological investigations, internal structures and microprobe analyses of zircons from Wadi Hawashiya granitoids, North Eastern Desert, Egypt. Final. Proc. 5th Int. Conf. Geol. Arab World (GAW5), Cairo Univ., Egypt, pp. 112–134.

El-Metwally, A.A., El-Aassy, I.E., Essawy, M.A., El-Mowafy, A.A., 1999. Petrological, structural and geochemical studies on the basement rocks of Gabal Um Zariq-Wadi Kid area, southeastern Sinai, Egypt. Egypt. J. Geol. 43 (1), 147–180.

El-Sheshtawy, Y.A., Abu El-Leil, I., 1989. Significance of zircon as a guide to the classification and genesis of some Egyptian granitic rocks. Mansoura Sci. Bull. 16, 371–391.

El-Sheshtawy, Y.A., Aly, M.M., Ahmed, A.M., 1988. Geochemistry and tectonic environments of the granite–pegmatite dykes around Wadi El-Markh area, Sinai, Egypt. Mansoura Sci. Bull. 15 (2), 205–226.

Folk, R.L., Ward, W.C., 1957. Brazos river bar: a study in the significance of grain size parameters. J. Sediment. Petrol. 27, 3–26.

Gilat, A., Shirav, M., Bogoch, R., Halicz, L., Avner, U., Nahlieli, D., 1993. Significance of gold exploitation in the Early Islamic period, Israel. J. Archaeol. Sci. 20, 429–437.

Gindy, A.R., 1961. On the radioactivity and origin of the manganese–iron deposits of west central Sinai, Egypt. Bull. Acad. Sci. Egypt, 71–86.

Herail, G., Lagos, J., Vivallo, W., 1999. Gold despersion in Andean

desert environments (Atacama, Chile). J. Geochem. Explor. 66, 427–439.

Jennex, L.C., Murphy, J.B., Anderson, A.J., 2000. Post-orogenic exhumation of an auriferous terrane: the paleoplacer potential of the Early Carboniferous St. Marys Basin, Canadian Applachians. Miner. Depos. 35, 776–790.

Kabesh, M.L., Refaat, A.M., Abdallah, Z.M., 1976. The significance of zircon as a guide to the petrogenesis of granites from Ras Barud area, Eastern Desert, Egypt. J. Univ. Kuwait, Sci. 3, 207–216.

Khalid, A.M., Oweiss, Kh.A., 1995a. Results of mineral exploration programs in southeastern Sinai, Egypt. Ann. Geol. Surv. Egypt 20, 207–220.

Khalid, A.M., Oweiss, Kh.A., 1995b. Geochemical exploration for gold at Wadi Kid area, southeastern Sinai, Egypt. Ann. Geol. Surv. Egypt 20, 333–342.

Levson, V.M., Blyth, H., 2001. Formation and preservation of a Tertiary to Pleistocene fluvial gold placer in northwest British Columbia. Quat. Int. 82, 33–50.

Moiala, R.J., Weiser, D., 1968. Texture parameters: an evolution. J. Sediment. Petrol. 38, 45–53.

Morad, S.A., Aldahan, A.A., 1986. Alteration of detrital Fe–Ti oxides in sedimentary rocks. Bull. Geol. Soc. Am. 97, 567–578.

Owens, M.R., 1987. Hafnium content of detrital zircons, a new tool for provenance study. J. Sediment. Petrol. 57, 830–842.

Petkovic, M., Babovic, O., 1995. Model of statistical data processing for alluvial deposits of gold. Geol. Soc. Greece Spec. Pap. 4, 810–813.

Pierce, J.W., Siegel, F.R., 1969. Quantification in clay mineral studies of sediments and sedimentary rocks. J. Sediment. Petrol. 39, 187–193.

Shimron, A.E., 1981. The Dahab mafic–ultramafic complex, Southern Sinai Peninsula, a probable ophiolite of Late Proterozoic (Pan-African) age. Israel Geol. Surv. 6, 161–164.

Surour, A.A., Kabesh, M.L., 1997. Calc-alkaline magmatism and associated mafic microgranular enclaves of Wadi Risasa area, southeastern Sinai, Egypt. Ann. Geol. Surv. Egypt 21, 35–45.

Takla, M.A., Hussein, A.A., 1995. Shield rocks and related mineralization in Egypt. The 11th Sympos. Precamb. and Develop., Cairo, Egypt, Abstract, 6–7.

Vavelidis, M., Melfos, V., Boboti-Tsitlakidou, I., Arikas, K., 1997. A new occurrence of placer gold in the Marathousa area (central Macedonia, Greece). In: Papunen, H. (Ed.), Mineral Deposits. Balkema, Rotterdam, pp. 335–338.